



HAL
open science

Coupling a hierarchy of diffuse interface models with kinetic-based moment methods for spray atomization simulations in cryogenic rocket engines

Pierre Cordesse, Angelo Murrone, Marc Massot

► **To cite this version:**

Pierre Cordesse, Angelo Murrone, Marc Massot. Coupling a hierarchy of diffuse interface models with kinetic-based moment methods for spray atomization simulations in cryogenic rocket engines. ICLASS 2018 14TH INTERNATIONAL CONFERENCE ON LIQUID ATOMIZATION & SPRAY SYSTEMS, Jul 2018, CHICAGO, United States. hal-01888477

HAL Id: hal-01888477

<https://hal.science/hal-01888477v1>

Submitted on 5 Oct 2018

HAL is a multi-disciplinary open access archive for the deposit and dissemination of scientific research documents, whether they are published or not. The documents may come from teaching and research institutions in France or abroad, or from public or private research centers.

L'archive ouverte pluridisciplinaire **HAL**, est destinée au dépôt et à la diffusion de documents scientifiques de niveau recherche, publiés ou non, émanant des établissements d'enseignement et de recherche français ou étrangers, des laboratoires publics ou privés.

Coupling a hierarchy of diffuse interface models with kinetic-based moment methods for spray atomization simulations in cryogenic rocket engines

P. Cordesse*, A. Murrone, M. Massot
ONERA, France and CMAP, Ecole polytechnique, France
pierre.cordesse@polytechnique.edu, angelo.murrone@onera.fr,
marc.massot@polytechnique.edu

Abstract

Jet atomizations play a crucial role in many applications such as in cryogenic combustion chambers, thus must be thoroughly studied to understand their impact on high-frequency instabilities. Since direct numerical simulations of these two-phase flows in a real configuration of an engine are still out of reach, predictive numerical tools must be developed using reduced-order models. However great care must be taken on the choices of these models in order to both have sound mathematics properties and lead to predictive simulations. The contribution of this work is three-fold. First, we present an original fully Eulerian modelling strategy. It relies on the coupling of a hierarchy of diffuse interface models with a Eulerian kinetic-based moment method (KBMM). Special attention will be given to the description of various disequilibrium levels for the diffuse interface model, which describes the separated and mixed zones. A member of the KBMM hierarchy will accurately describe the polydisperse evaporating spray generated through atomization. Second, to cope with the strong discontinuities encountered in jet atomization, a robust and accurate numerical method using multi-slope MUSCL technique will be applied. The extension of the proposed strategy to the various levels of the diffuse interface models will be discussed. Third, relying on the previous two points, large eddy simulations of a jet atomization in a cryogenic combustion chamber in subcritical conditions are presented using various levels of modelling.

Introduction

In a cryogenic combustion chamber, the multi-scale and various physical phenomena are very complex and their interaction is a current research area. In particular, the primary atomization plays a crucial part in the way the engine works, thus must be thoroughly studied to understand its impact on high-frequency instabilities. The latter have been encountered in the past and can lead to critical damages of the rocket. Even though experimentations must be conducted to enable simulation validation and to understand the observed physical phenomena, predictive numerical simulations are mandatory, at least as a complementary tool to understand the physics and even more to conceive new combustion chambers and predict instabilities they may generate in a given configuration. In subcritical conditions, downside a coaxial injector, the liquid oxygen atomization by co-current gaseous hydrogen engenders three two-phase flow topologies : at the exit of the injector, the two phases are separated by an interface. Downstream a polydisperse spray of droplets is carried by the gaseous phase. In between, shear stress caused by strong velocity gradients tears the liquid core apart and ligaments are formed. This process is called primary atomization. The ligaments get thinner and thinner until they break into droplets. In this *mixed region*, the subscale physics and the topology of the flow are very complex. Direct numerical simulations of these two-phase flows in a real engine configuration are still out of reach, CPU needs being too high and defining the smallest scale of a two-phase mixture is still unclear. Therefore predictive numerical tools must be developed using reduced-order models. However great care must be taken on the choices of these models in order to both have solid mathematics properties leading to robust and accurate numerical simulations after a validation process. Two main strategies are encountered in the literature to build such reduced-order models :

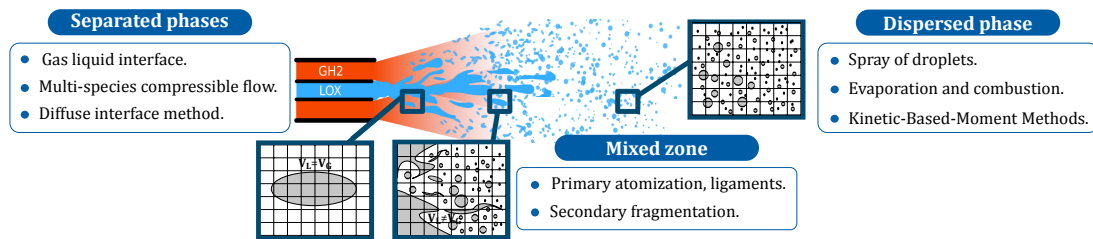
- **Coupled models:** a first model is used in the separated-phase can be derived either by statistical averaging of the instantaneous Navier-Stokes equations for each phase [7] or by front tracking methods including some level of space filtering [14]. In the dispersed-phase zone, the polydispersity in size, velocity and temperature of the droplets is taken into account with different methods: tracking the particles in a Lagrangian way [26], or using an Eulerian approach where the droplets distribution is rebuilt thanks to the method of moments [23]. Usually, the methods applied to the separated phase zone are extended to *the mixed region*, but it implies either a high level of the phase disequilibrium description or an extremely refined mesh. On a top that, a numerical strategy must be provided to communicate informations between the different models.

*Corresponding author: pierre.cordesse@polytechnique.edu

- **Unified models:** In this strategy, a unique model takes care of all the flow topologies without the need of model coupling methods. A recent proposal in this spirit can be found in [8], where a unified model accounting for micro-inertia and micro-viscosity associated to bubble pulsation is proposed. The objective is here to model the sub-scale using a unified description, which degenerate into a predictive spray model in the disperse flow area [11] [10].

The present work aims at using the first approach by coupling a diffuse interface method to a member of the kinetic based moment methods (KBMM). The two models transport different variables. Therefore they need to be coupled in some way, transporting the information from one zone of the domain to the other. A reference implementation of the coupled approach can be found in [16], but the prediction of the polydispersity of the generated spray has to rely on some parameters impacting the resulting structure of the spray. The two-fluid model used, called a *four-equation model* is not capable of describing the phase disequilibria in terms of temperature, velocity and pressure. Even if simulations including a temperature disequilibrium have already been conducted on real configurations, it seems it has never been done with also a velocity disequilibrium [21]. Figure 1 illustrates the numerical strategy applied in this work.

Figure 1: Topologies of a cryogenic jet atomization in sub-critical conditions.



The paper is organized as follows. First, a mathematical overview of the various models used is addressed. The numerical methods applied to these models are described in the following section. Later on details of the numerical simulations conducted are given and a comparison between the different models is drawn to finally conclude on the work.

Mathematical modeling

Two models are used: a two-phase flow model based on diffuse interface methods and a multi-fluid model derived by Kinetic Based Moment Methods. They are two-way coupled.

Hierarchy of diffuse interface methods

Diffuse interface methods rely on the assumption that at any time t , at any place x in a given domain Ω , two phases can coexist. Hence, three configurations occur : time-space point (t, x) with only one or the other phase or with both of them. The latter forms a mixture. To obtain a continuum-mechanical approach for describing two phase flows, a statistical averaging process is applied on the microscopic Navier-Stokes equations for each phase [7]. A system of conservative equations is obtained allowing full disequilibrium between the two phases. Two assumptions are made to obtain these conservation equations. First, each phase behaves independently to one another, the exchanges between the phases are modeled by additional mass, momentum and energy exchange terms. Second, the mixture follows the same conservation equations obtained by summing those of each phase. Then, the entropy inequality derived from the second law of thermodynamics imposes restrictions on the constitutive equations, resulting in models for each exchange term. However the system of six equations, namely a mass, momentum and energy equations for each phase, is not closed. Baer and Nunziato introduced for the first time a supplementary evolutionary equation for the volume fraction of one phase to ensure the model closure, resulting in a so-called *seven-equation model* describing the deflagration-to-detonation (DDT) in gas-permeable, reactive granular materials [2]. This model has been generalized for two-phase flow by introducing two interfacial quantities, u_I and p_I , the averaged interfacial velocity and pressure respectively [19], and writes in a quasi-linear form :

$$\partial_t \mathbf{U} + A_1 \partial_x \mathbf{U} = \frac{\mathbf{R}(\mathbf{U})}{\epsilon} + S_{u \rightarrow q} - S_{drag} - S_h \quad (1)$$

with the conservative variables $\mathbf{U} = (\alpha_2, \mathbf{U}_2, \mathbf{U}_1)^t$, $\mathbf{U}_k = (\alpha_k \rho_k, \alpha_k \rho_k u_k, \alpha_k \rho_k E_k)^t$, the conservative fluxes $\mathbf{F}(\mathbf{U})$ and the non-conservative fluxes $\mathbf{G}(\mathbf{U})$ defining the matrix A_1 as:

$$A_1 = \begin{pmatrix} u_I & 0 & 0 \\ \partial_{\alpha_2} \mathbf{F}(\mathbf{U}_2) + \mathbf{G}(\mathbf{U}_2) & \partial_{\mathbf{U}_2} \mathbf{F}(\mathbf{U}_2) & 0 \\ \partial_{\alpha_2} \mathbf{F}(\mathbf{U}_1) + \mathbf{G}(\mathbf{U}_1) & 0 & \partial_{\mathbf{U}_1} \mathbf{F}(\mathbf{U}_1) \end{pmatrix} \quad (2)$$

where $\mathbf{F}(\mathbf{U}_k) = (\alpha_k \rho_k u_k, \alpha_k \rho_k u_k^2 + \alpha_k p_k, \alpha_k (\rho_k E_k + p_k) u_k)^t$ and $\mathbf{G}(\mathbf{U}_2) = -\mathbf{G}(\mathbf{U}_1) = (0, p_I, p_I u_I)^t$. α_k is the volume fraction of phase $k = 1, 2$, ρ_k the partial density, u_k the phase velocity, p_k the phase pressure, $E_k = \epsilon_k + 1/2 u_k^2$ the total energy per unit of mass, ϵ_k the internal energy. A two-parameter equation of state associated with a Gibbs law will be used hereafter. Mass transfer between the two phases is neglected. $S_{u \rightarrow q}$ models the atomization of the liquid phase into droplets and the pseudo coalescence of the droplets into the liquid phase, S_{drag} the drag force of the gas acting upon the droplets, S_h the conducto-convective heat transfer at the surface of the droplet.

Because a mixture can not stay in full disequilibrium, \mathbf{R} is an application describing the mechanical, hydrodynamic and thermal relaxations between the two phases and ϵ is the characteristic time for each of these processes. The condition $\mathbf{R}(\mathbf{U}) = 0_{\mathbb{R}^7}$ imposes three constraints (pressure, velocity and temperature equilibria) and defines the constrained manifold $\mathcal{E} = \{\mathbf{U} \in \mathbb{R}^7, \mathbf{R}(\mathbf{U}) = 0_{\mathbb{R}^7}\}$. Usually, the constraint \mathbf{R} is defined by physical processes respecting the entropy inequality. When only pressure and velocity relaxations are accounted for, it decomposes classically onto

$$\frac{\mathbf{R}}{\epsilon} = \frac{\mathbf{R}^u}{\epsilon_u} + \frac{\mathbf{R}^p}{\epsilon_p}, \text{ with } \frac{\mathbf{R}^u}{\epsilon_u} = \left(0, \frac{\mathbf{R}_2^u}{\epsilon_u}, \frac{\mathbf{R}_1^u}{\epsilon_u}\right)^t \text{ and } \frac{\mathbf{R}^p}{\epsilon_p} = \left(\frac{p_2 - p_1}{\epsilon_p}, \frac{\mathbf{R}_2^p}{\epsilon_p}, \frac{\mathbf{R}_1^p}{\epsilon_p}\right)^t \quad (3)$$

where $\mathbf{R}_2^u = -\mathbf{R}_1^u = (0, u_2 - u_1, u_I(u_2 - u_1))$, $\mathbf{R}_2^p = -\mathbf{R}_1^p = (0, 0, p_I(p_2 - p_1))$. The interfacial terms u_I and p_I modeling varies and an expression for the relaxation parameters ϵ_u and ϵ_p have been for example derived using the DEM technic in [20]. Relaxing the pressure and the velocity can be interpreted as projecting the full disequilibrium state $\mathbf{U} \in \mathbb{R}^7$ on the constraint manifold \mathcal{E} where the relaxation $\mathbf{R}(\mathbf{U}) = 0_{\mathbb{R}^7}$ occurs. One can thus look for a reduced model by projecting $\mathbf{U} \in \mathbb{R}^7$ on \mathbb{R}^p , $p \leq 7$. It can be shown that there exists an admissible map M from \mathbb{R}^p to $\mathcal{E} \subset \mathbb{R}^7$ which leads to semi-stable systems. In particular, one can obtain the *five-equation model* where the phases have now the same pressure and the same velocity. In [18], the authors interpret the reduced model as the asymptotic limit of the *seven-equation model* when $\epsilon \rightarrow \infty$. Following their lines, without the coupling source terms, the *five-equation model* writes :

$$\partial_t \mathbf{U} + A_1 \partial_x \mathbf{U} = \frac{\mathbf{R}(\mathbf{U})}{\epsilon} \quad (4)$$

with the conservative variables $\mathbf{U} = (\alpha_2, \mathbf{U}_2, \mathbf{U}_1)^t$, $\mathbf{U}_k = (\alpha_k \rho_k, \alpha_k \rho_k u, \alpha_k \rho_k E_k)^t$, the conservative fluxes $\mathbf{F}(\mathbf{U}_k)$ and the non-conservative fluxes $\mathbf{G}(\mathbf{U}_k)$ defining the matrix A_1 as in Equation (2) but with $u_I = u_1 = u_2 = u$, $p_I = p_1 = p_2$. Finally taking the Taylor series of the relaxing source terms with respect to ϵ gives $u_I = u + o(\epsilon)$, $p_I = p + o(\epsilon)$ and

$$\frac{u_2 - u_1}{\epsilon_u} = \frac{\alpha_1 \rho_1 \alpha_2 \rho_2}{\rho} \left(\frac{1}{\rho_1} - \frac{1}{\rho_2} \right) \partial_x p + o(\epsilon) \quad \frac{p_2 - p_1}{\epsilon_p} = \alpha_1 \alpha_2 \frac{\rho_1 a_1^2 - \rho_2 a_2^2}{\sum_{k=1,2} \alpha_{k'} \rho_k a_k^2} \partial_x u + o(\epsilon) \quad (5)$$

where ρ is the mixture density $\rho = \alpha_1 \rho_1 + \alpha_2 \rho_2$, a_k is the phase sound of speed, $a_k^2 = \partial p_k / \partial \rho_k|_{s_k}$, and $k' = k + 1[2]$. The zero order terms are injected into Equation (3) to define \mathbf{R} in Equation (4). In practice, for the *five-equation model*, the two partial momentum and energy equations are summed and replaced by an equation on the total momentum ρu and an equation on the total energy ρE respectively. Only one relaxing term remains in the system of equation: that of the volume fraction equation. Thus the only difference between the *five-equation model* and the *instantaneously relaxed seven-equation model* lies in the volume fraction equation.

When relaxing the temperatures, one obtains the compressible Navier-Stokes equations, called also *four-equation model*. This last model, associated with the two previous one, defines the hierarchy of diffuse interface models at disposal.

To accurately describe the *mixed region*, one needs to use the out-of-equilibrium *seven-equation model* to feed more accurately the KBMM for the velocity, temperature and pressure of the droplets.

Mathematical properties of the seven-equation model

The mathematical properties of the *seven-equation model* have been studied by [4] among others. It is hyperbolic and admits 7 eigenvalues $\text{Sp}(A_1) = \left\{ u_I, \{u_k, u_k \pm a_k\}_{k=2,1} \right\}$. As noticed by [9], the system becomes non strictly hyperbolic when two or more eigenvalues coincide. Assuming the interface velocity u_I is defined as a linear average of the two phase velocities $u_I = \beta u_1 + (1 - \beta)u_2$, $\beta \in [0, 1]$ then the eigenvalues $\lambda_1 = u_I$, $\lambda_2 = u_2$ and $\lambda_5 = u_1$ remain distinct. Thus the only condition leading to hyperbolic degeneracy, designated as the *non resonance condition* in [5], is $(u_k - u_I)^2 = a_k^2$, $k = 1, 2$.

A KBMM element: sampling method

It would have been possible to choose one of the best KBMM element such as a multi-fluid modelling using a continuous discretization of the droplet size through sections, which has been validated on evaporating polydisperse sprays [23]. Nevertheless since our primary concern is to increase the disequilibrium in the interface diffuse model, for sake of simplicity, a simple KBMM element has been chosen: a multi-fluid modelling with sampling methods [15] and monokinetic and monotemperature assumptions. Evaporation and coalescence of the droplets are neglected, thus only one sample of droplet is needed to attest the success of the coupling strategy of the two models. The system of equation is weekly hyperbolic [6] and writes for one class:

$$\partial_t \mathbf{Q} + \partial_x F_q(\mathbf{Q}) = S_{drag} + S_h + S_{q \rightarrow u} \quad (6)$$

where the variables are $\mathbf{Q} = (n, \alpha_d \rho_d, \alpha_d \rho_d \mathbf{u}_d, \alpha_d \rho_d \epsilon_d)^t$ the conservative fluxes $F_q(\mathbf{Q}) = (n \mathbf{u}_d, \alpha_d \rho_d \mathbf{u}_d, \alpha_d \rho_d \mathbf{u}_d^2, \alpha_d \rho_d \epsilon_d \mathbf{u}_d)^t$, and the coupling source term $S_{q \rightarrow u}$. n is number of droplets, ρ_d is the liquid density depending only on the temperature, \mathbf{u}_d the droplet velocity, ϵ_d the droplet internal energy. To be conservative, the coupling source terms of Equation (1) and Equation (6) must balance out each other, thus $S_{q \rightarrow u} = -S_{u \rightarrow q}$.

Numerical methods

The models used hereafter to simulate the jet atomization have been implemented in the CEDRE software which is a multi-physics platform working on general unstructured meshes and organized as a set of solver [13]. Two solvers are used, *SEQUOIA* for the diffuse interface model and *SPIREE* for the KBMM. Both are two-way coupled by the source terms $S_{q \rightarrow u}$ and $S_{u \rightarrow q}$ exchanged at every time step. A Lie splitting technic is used resulting in the following system of equations:

$$\mathbf{U}^{n+1} = \left[S_{u \rightarrow q} - S_h - S_{drag} \frac{\mathbf{R}^u}{\epsilon_u} \right]^{\Delta t} \frac{\mathbf{R}^p}{\epsilon_p} \mathcal{H}_u(\mathbf{U}^n) \quad \mathbf{Q}^{n+1} = [S_{q \rightarrow u} S_h S_{drag}]^{\Delta t} \mathcal{H}_q(\mathbf{U}^n) \quad (7)$$

The hyperbolic operators \mathcal{H}_u and \mathcal{H}_q corresponding to convection of the two-phase model and the dispersed model respectively, are calculated using an approximate Riemann solver, HLLC, and a Pressureless Gas Dynamics exact Riemann solver respectively [3]. Then relaxation operators and source terms are applied in the order showed in Equation (7) to define the new states \mathbf{U}^{n+1} and \mathbf{Q}^{n+1} of the conservative variables.

HLLC scheme for the two-phase flow model

Ideally, an exact Riemann solver should be able to solve the hyperbolic operator \mathcal{H}_u [22], however the computational cost is way too expensive. Thanks to hyperbolicity of the model, a VFRoe solver has been tested [1] using primitive variables $\mathbf{U} = (\alpha_1, \rho_1, \mathbf{u}_1, p_1, \rho_2, \mathbf{u}_2, p_2)^t$. Nevertheless, it was not robust enough to handle the strong gradients occurring in the chamber. Therefore, choice has been made to use a HLLC solver which shows usually good robustness [24]. Other difficulties for solving Equation (1) are owed to the non-conservative terms and modelling the interfacial terms. The approach proposed in [12] tackles all the issues by assuming (1) the interfacial terms p_I and u_I to be local constants in the Riemann problem, (2) the volume fraction to vary only across the interfacial contact discontinuity u_I . As a result, the non conservative terms in Equation (1) vanish, u_I and p_I are determined locally by Discrete Equation Method (DEM) [20] at each time step and stay constant during the update. Thus, phases are now decoupled and Equation (1) splits into two conservative sub-systems to which a classic HLLC solver is applied. As proposed by [12], a second order reconstruction is developed. It uses the MUSCL-Hancock strategy but the spatial reconstruction is done with a multi-slope MUSCL scheme developed by [17]. Finally, two slope limiters have been tested: the Van-Leer limiter and a hybrid limiter developed in

[16], which combines the advantages of a CFL-Superbee limiter for high gradient regions and a third order CFL dependent limiter for the regular regions.

Relaxation procedure

In many applications, the pressures of a two-phase flow are assumed to relax instantaneously. Thus, after the hyperbolic update, the following ODE is solved: $\partial_t \mathbf{U} = \mathbf{R}^p(\mathbf{U})/\epsilon_p$, with $\epsilon_p \rightarrow \infty$ which infers u_k remain constant. Manipulating the equations, an equilibrium pressure is obtained by solving a second order equation with an iterative procedure such as a Newton method. Detailed of the equation can be found in [12]. As for the velocities, within the context of assisted jet atomization in sub-critical conditions, the relaxation time is finite. The following ODE is solved: $\partial_t \mathbf{U} = \mathbf{R}^u(\mathbf{U})/\epsilon_u$ which implies α_k, ρ_k are conserved during the relaxation. Subtraction of the momentum equations gives the following ODE on the split velocity $u_d = u_2 - u_1$: $\partial_t u_d - A^o u_d/\epsilon_u = 0$ where superscript o denotes the state before relaxation. A first numerical approach is to fix a remaining slip velocity ratio target at each computational time step Δt . It defines the characteristic relaxing time:

$$\frac{\epsilon_u}{A^o} = \ln(X)\Delta t \text{ with } X = \frac{u_d(\Delta t)}{u_d^o} \text{ and } A^o = \frac{\alpha_1^o \rho_1^o + \alpha_2^o \rho_2^o}{\alpha_1^o \rho_1^o \alpha_2^o \rho_2^o} \quad (8)$$

An instantaneous velocity relaxation is in practice also possible and manipulating the ODE leads to a unique relaxed velocity, which is the mass weighted average of the two velocities before relaxing.

Coupling source terms

The physical processes accounted for in the coupling source terms are the atomization of the liquid phase, S_{atom} , and the pseudo-coalescence of the liquid droplets, S_{coal} , defined respectively as $S_{atom} = \alpha_2 \rho_2 f_{atom} \lambda_{atom}$ and $S_{coal} = \alpha_d \rho_d f_{coal} \lambda_{coal}$ where f_{atom} is the atomization frequency, λ_{atom} describes the efficiency of the atomization, f_{coal} the pseudo-coalescence frequency and λ_{coal} the pseudo-coalescence efficiency, defined all in [16]. Thanks to the increase of disequilibrium by using the *seven-equation model* with finite velocity relaxation, S_{atom} has been revisited making full use of the existence of two velocities to track regions with high shear stress and thus regions where atomization should occur.

Results and Discussion

In the following, numerical simulations are performed on a subcritical cryogenic single-injector configuration using the hierarchy of diffuse interface models introduced previously, namely the *five equation model (5eq)*, the *instantaneously relaxed seven equation model (IR7eq)* and the *non-instantaneously relaxed seven equation model (NIR7eq)*. On the way to validation of the numerical results with experimental data, the first interest is to attest the robustness of the numerical method by increasing difficulties one step at a time: first increase the disequilibrium of the diffuse interface model then activates the coupling via atomization and pseudo-coalescence source terms. Doing so, we can study properly the impact of the models and the coupling on quantities of interest such as the liquid core length, its dynamics, the sharpness of the interface and the velocities at the interface. However, we choose operating conditions as close as possible to a real configuration, the results may thus also be predictive.

Description of the configuration

The configuration choice meets several criteria. First, the geometry mimics the experimental test-bench MAS-COTTE [25], a cryogenic rocket engine combustion chamber. It adopts a unique co-axial injector of liquid oxygen $O_2(l)$ circumscribed by gaseous hydrogen $H_{2(g)}$. Second, it must offer three dimensions in space to capture the dynamics of the jet. However, the computational time should not be too heavy to conduct numerical tests and validations. Hence, only a portion $\theta \in [0, \pi/3]$ of the cylindrical chamber is meshed making use of the symmetric axis of the cylinder preventing the liquid jet to flap. As seen in Figure 2, the mesh is refined inside the injector and at its exit where the liquid core flows in order to capture the interface dynamics. The mesh size is around a million tetra cells. The injector lip of length L^{lip} is meshed by four cells at the minimum mesh size Δx_{min} . Walls are set to adiabatic slip boundaries, the variables $(\rho_k, u_k, T_k, \alpha_k)$ define the inlets, the outlet is pressure defined at p_∞ . Table 1 summarizes key values of the configuration. The numerical simulation has been conducted as followed: first, the oxygen and the hydrogen have been injected with a ramp-up to reach at $\tau = \tau_0$ the operating point using

Figure 2: Geometry and mesh of the configuration

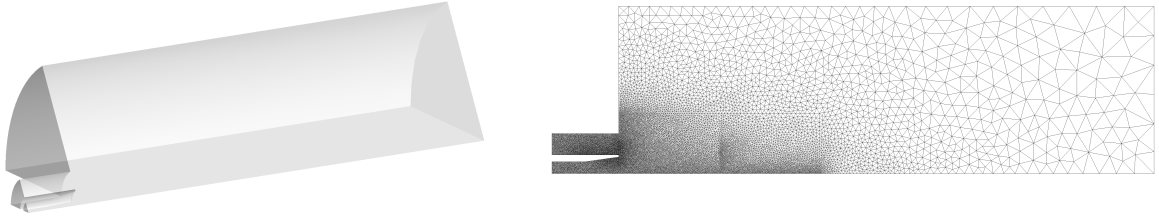



Table 1: Physical parameters of the configuration

$J = \frac{\rho_1 u_1^2}{\rho_2 u_2^2}$	T_1/T_2	Gas	Liquid	$L^{\text{lip}}/\Delta x_{\text{min}}$	p^∞	ϵ_α
~ 3	~ 3	$H_{2(g)}$	$O_{2(l)}$	4	10 bar	10^{-6}

the *5eq* with no coupling. Then, the simulation has run approximately ten times the characteristic convective time of the liquid core τ_{conv} . At this point, designated τ_1 , start the comparisons of the models.

Case 1 : comparison of the five-equation model and the instantaneously relaxed seven-equation model without atomization

The first case aims at comparing the *5eq* with the *IR7eq*. The unique difference emphasized by the mathematical study lies on the order with respect to ϵ of the source term of the volume fraction equation. Therefore Figure 3 compares qualitatively the liquid core obtained after two τ_{conv} simulation time starting at $\tau = \tau_1$. Looking at

Figure 3: Comparison of the liquid volume fraction α_2 : slice at $\theta = \pi/6$, at $\tau = \tau_1$ (left) and $\tau = \tau_1 + 2\tau_{\text{conv}}$ (right), $\alpha_2 = 1.0$  $\alpha_2 = 0.01$

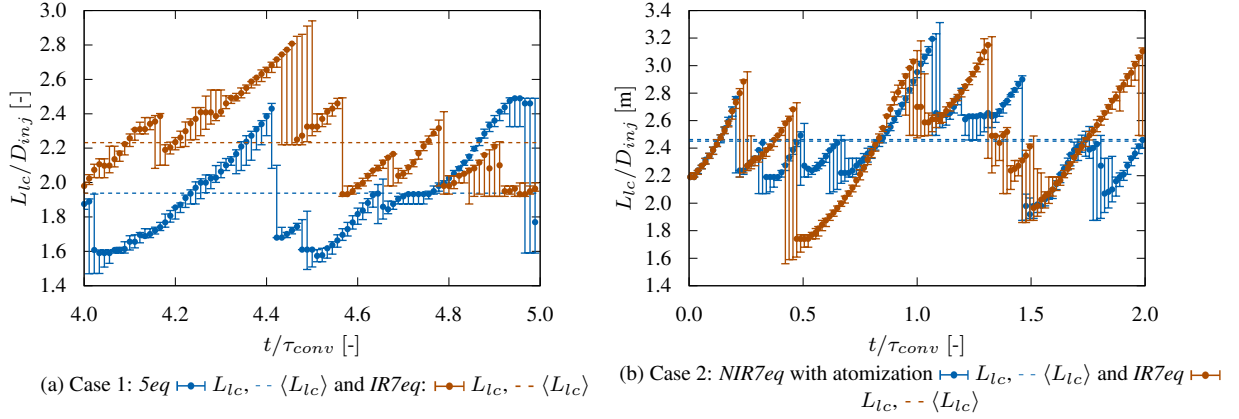


the right figure, the outlook of the interface above and below the axis looks quite unchanged at first sight. The models capture the disruption of the interface due to high-shear stress sparking ligaments. The interface seems less diffusive in the region close to the liquid injector outlet for the *IR7eq*. Since the sound speeds involved in the spectrum of the two models are different, the CFL condition writes not the same. Thus, for a identical CFL constraint, the time step is about 25% smaller for the latter model explaining potentially the diminution of diffusion. Furthermore we focus on quantitative results. The length of the liquid core, L_{lc} , made dimensionless by the diameter of the $O_{2(l)}$ injector outlet, D_{inj} , is plotted over time scaled by τ_{conv} in Figure 4a along with its time average $\langle L_{lc} \rangle$. The oscillations of the length reveal a pulsating movement along the axial direction. Even after $4\tau_{\text{conv}}$, the behaviour of the liquid core is similar for the two models. Only the average length over time $\langle L_{lc} \rangle$ for the *IR7eq* is 15% greater than for the *5eq*. It can be interpreted as a quantitative argument attesting of a less-diffusive interface in the case of the *IR7eq*, again certainly due to the gain on accuracy on the volume fraction equation and a smaller time step. Nevertheless, putting aside the dissimilarities on the volume fraction, the *IR7eq* does not offer significant improvement compared to the *5eq*.

Case 2 : comparison of the instantaneously relaxed seven-equation model and the non-instantaneously relaxed seven-equation model with atomization

To better describe the flow in the region close to the interface, it is necessary to increase the disequilibrium of the phases. In the present configuration, a strong velocity gradient occurs at the interface, and the ratio of kinetic energy, $J = (\rho_1 u_1^2)/(\rho_2 u_2^2)$, is about 3. Physically, the liquid is expected to be accelerated by the gas, but not instantaneously. Therefore it is physically wrong to assume an instantaneous relaxation time for the velocities of the phase. The same comment can be done on the temperatures. So far in the literature [21], it has been achieved to

Figure 4: Model influence on the liquid core length L_{lc} over time and its time average $\langle L_{lc} \rangle$ at isovalue $\alpha_2=0.95\pm 0.04$. Figure 4a compares *5eq* and *IR7eq*. Figure 4b compares *NIR7eq* and *IR7eq*



allow the phases to have their own temperature but always have a common velocity using for example the *5eq*. Even when the *7eq. model* has been used, it was always with an instantaneous relaxation time of the velocities mainly due to numerical difficulties [12]. In such case, the *7eq. model* lacks of interest in practice compared to the *5eq*. Here for the first time, we have successfully conducted a simulation of jet atomization with a *non-instantaneously relaxed seven-equation model*. Each phase retains its own velocity in the region of the interface. The simulation has run for $2.5\tau_{conv}$ attesting the success of the implementation. Figure 5 presents the volume fraction of liquid droplets α_d and the norm of the slip velocity in the two-phase flow $|\mathbf{u}_{slip}|$. The slip velocity is highly concentrated

Figure 5: *NIR7eq* with atomization (Legend: blue isovolume of $\alpha_2 = 0.99$, volume fraction of droplets in the SPIREE solver α_d , slip velocity norm $|\mathbf{u}_{slip}|$)



in the interface region, on the so-to-say "gaseous side", where atomization occurs. It permits to give to the atomized liquid droplets the speed of the liquid phase. It is a major gain of accuracy as long as the characteristic time of velocity relaxation is physically well-defined. At the present time, the characteristic time is finite and constant, but it will be revisited in future works to match physical reality. Finally, a comparison between the *IR7eq* and no coupling and the *NIR7eq* with atomization is proposed hereafter. The reason why the former was not coupled with atomization is due to the fact that the atomization source term $S_{u \rightarrow q}$ depends on the existence of a slip velocity u_d . Nevertheless comparing these two models helps us to verify that the activation of the atomization does not destroy the liquid core. Figure 6 compares qualitatively the liquid interface after $1.5\tau_{conv}$ simulation time. Interestingly,

Figure 6: Comparison of the liquid volume fraction α_2 : slice at $\theta=\pi/6$, at $\tau=\tau_1$ (left) and $\tau=\tau_1+1.5\tau_{conv}$ (right), $\alpha_2=1.0$ \rightarrow $\alpha_2=0.01$



the appearance is similar for the two models meaning the atomization process is not interfering with the liquid core, which is what was expected based on the choice of the efficiencies of S_{atom} and S_{coal} . Furthermore the length of the liquid core L_{lc} is also very similar up to the point that the two models show the same time averaged length (Figure 4b) which confirms that the atomization procedure has been carefully implemented.

Conclusion and future prospects

An original fully Eulerian modelling strategy of jet atomization in sub-critical combustion chambers has been successfully implemented. First, it relies on the coupling of a hierarchy of diffuse interface models from a *five-equation model* to a *non-instantaneously relaxed seven-equation model* with an eulerian model derived by kinetic-based moment method (KBMM). Temperature and velocity disequilibrium levels for the diffuse interface model have been included to describes the separated and mixed zone. The numerical strategy has copped with the strong discontinuities encountered in jet atomization thanks to a robust and accurate numerical method using multi-slope MUSCL technique. All the models have captured the pulsating movement of the liquid core and the distortion of the interface due to high-shear stress. The *seven-equation model* when non-instantaneously relaxed, has permitted to feed the KBMM element with a liquid velocity.

In future works, we will first aim at defining a physical dynamic velocity relaxation time. Then, we will couple the diffuse interface model with a more accurate KBMM element such as multi-sectional models including coalescence and evaporation source terms to obtain a predictive spray of droplets and compare it to experimental data obtained on the test-bench MASCOTTE [25].

Acknowledgments

This work has been cofunded by the French Aerospace Lab (ONERA) and the French Government Space Agency (CNES). Simulations have been successfully conducted using the CEDRE computational fluid dynamic software.

References

- [1] Andrianov, N., Saurel, R., and Warnecke, G., *Int. J. Numer. Meth. Fl.* 412:109–131 (2003).
- [2] Baer, M. R. and Nunziato, J. W., *Int. J. Multiphase Flow* 126:861–889 (1986).
- [3] Boileau, M., Lagarde, J., Dupif, V., Laurent, F., and Massot, M., *ICMF Proceedings, Firenze, Italy.* (May 2016).
- [4] Coquel, F., Gallouët, T., Hérard, J.-M., and Seguin, N., *C.R. Math.* 33410:927–932 (2002).
- [5] Coquel, F., Hérard, J.-M., Saleh, K., and Seguin, N., *Commun. Math. Sci.* 12:593–600 (2014).
- [6] De Chaisemartin, S., Fréret, L., Kah, D., Laurent, F., Fox, R., Reveillon, J., and Massot, M., *Comptes Rendus Mécanique* 3376:438–448 (2009).
- [7] Drew, D., *Annu. Rev. Fluid Mech.* 15:291–291 (1983).
- [8] Drui, F. PhD Thesis. Université Paris-Saclay, July 2017.
- [9] Embid, P. and Baer, M., *Cont. Mech. Therm.* 44:279–312 (1992).
- [10] Essadki, M., De Chaisemartin, S., Laurent, F., and Massot, M. in revision to SIAP. 2018.
- [11] Essadki, M., De Chaisemartin, S., Massot, M., Laurent, F., Larat, A., and Jay, S., *Oil & Gas Science and Technologie, Rev. IFP Energies nouvelles* 715:25 (2016).
- [12] Furfaro, D. and Saurel, R., *Computers & Fluids* 111:159–178 (2015).
- [13] Gaillard, P., Le Touze, C., Matuszewski, L., and Murrone, A., *AerospaceLab* 11:16 (2016).
- [14] Hecht, N. PhD Thesis. INSA de Rouen, Mar. 2016.
- [15] Laurent, F. and Massot, M., *Combust. Theor. Model.* 54:537–572 (2001).
- [16] Le Touze, C. PhD Thesis. Université Nice Sophia Antipolis, 2015.
- [17] Le Touze, C., Murrone, A., and Guillard, H., *J. Comput. Phys.* 284:389–418 (2014).
- [18] Murrone, A. and Guillard, H., *J. Comput. Phys.* 202:664–698 (2005).
- [19] Saurel, R. and Abgrall, R., *J. Comput. Phys.* 1502:435–467 (Apr. 1999).
- [20] Saurel, R., Gavriluk, S., and Renaud, F., *J. Fluid Mech.* 495:283–321 (2003).
- [21] Saurel, R. and Pantano, C., *Annu. Rev. Fluid Mech.* 501:105–130 (2018).
- [22] Schwendeman, D., Wahle, C., and Kapila, A., *J. Comput. Phys.* 2122:490–526 (2006).
- [23] Sibra, A., Dupays, J., Murrone, A., Laurent, F., and Massot, M., *J. Comput. Phys.* 339:210–246 (2017).
- [24] Toro, E., Spruce, M., and Speares, W., *Shock Waves* 41:25–34 (1994).
- [25] Vingert, L., Habiballah, M., and Traineau, J., *EAC Proceedings, Paris, France.* (1999).
- [26] Zamansky, R., Coletti, F., Massot, M., and Mani, A., *J. Fluid Mech.* 809:390–437 (2016).